International Symposium
On Turbulence and Shear Flow
Phenomena (TSFP-9)
June 30 - July 3, 2015 *Melbourne, Australia*

TURBULENCE MODIFICATION IN POLYDISPERSE, WALL-BOUNDED TURBULENCE

David Richter
Department of Civil and Environmental
Engineering and Earth Sciences
University of Notre Dame
Notre Dame, IN, USA
David.Richter.26@nd.edu

Omar Garcia
Department of Civil and Environmental
Engineering and Earth Sciences
University of Notre Dame
Notre Dame, IN, USA

Christopher Astephen
Department of Civil and Environmental
Engineering and Earth Sciences
University of Notre Dame
Notre Dame, IN, USA

ABSTRACT

Direct numerical simulations of turbulent planar Couette flow are performed with Lagrangian point particles chosen to represent noninteracting, two-way coupled particles in low volume concentration, moderate mass concentration systems. Specifically, the behavior of polydisperse mixtures of small particles in wall-bounded turbulent flow is examined in terms of the ability of the dispersed phase to carry momentum alongside (and in place of) the turbulent carrier-phase Reynolds stress. It is shown that for binary mixtures of particles with distinct Stokes numbers, particle stresses are nearly additive, indicating that the presence of one size of particle does not influence the ability of another to couple with the flow. This result is generalized by performing an additional simulation with a continuous distribution of particle size, where it is again suggested that particles with acceleration timescales near that of the Reynolds-stress-producing motions at the wall dominate the balance, and that particles with larger Stokes numbers are similar in their limited ability to carry momentum across the domain. In the context of the low volume concentration, small particle assumptions, this has favorable consequences for modeling efforts.

INTRODUCTION

Multiphase and particle-laden flows are ubiquitous across a wide range of environmental and engineering processes, and oftentimes the small-scale interactions between phases play critical roles in determining important bulk-scale behavior. One example of this is the phenomenon of turbulence modification by a dispersed phase, where general statements about the ability and degree to which small particles modify turbulent flows remain elusive since the bulk-scale modification to turbulence statistics depends on the collective effect of direct interactions between individual particles and the surrounding turbulence (Balachandar & Eaton, 2010; Tanaka & Eaton, 2008; Gore & Crowe, 1989). This emphasizes the need for understanding the dependence of two-way coupling on particle characteristics and flow type. In this context, the present study is broadly motivated by natural flows where droplets or sand particles are suspended in the atmospheric boundary layer, where an underlying question is whether or not the presence of these constituents modifies the turbulent fluxes of momentum and scalars to/from the surface. The answer to this question has profound impacts on large-scale processes such as hurricane development (Andreas, 2011; Bao *et al.*, 2011) and bedform evolution (Bennett *et al.*, 2013), but also has general engineering significance.

A wide range of particle-laden simulations and experiments in turbulent flows have demonstrated a strong sensitivity of turbulence modification to, among other properties, particle inertia, as described by the dimensionless particle Stokes number (Balachandar & Eaton, 2010; Richter & Sullivan, 2013; Ferrante & Elghobashi, 2003; Kulick *et al.*, 1994). By changing the ability of particles to preferentially concentrate within turbulent flows, particle inertia plays an important role in determining the degree and nature of turbulence modification in wall-bounded flows. For example, particles which can preferentially concentrate on scales associated with near-wall vortices greatly weaken these motions through direct momentum and kinetic energy exchange, which modifies both the carrier phase and dispersed phase Reynolds stresses at the wall (Richter & Sullivan, 2014). Particles with larger (or smaller) Stokes numbers, on the other hand, remain more homogeneously mixed throughout the flow and cannot attenuate turbulent fluctuations as efficiently, yet still exhibit varying degrees of Reynolds stress modification.

While experimental investigations of particle-laden turbulence are essential to understanding two-way coupling, numerical studies of dispersed phase turbulence flow are, under certain conditions, uniquely equipped to provide in-

sight, detail, and resolution which is unavailable to laboratory observation. As with any numerical representation of a physical process, however, idealizations must always be made, and a common approximation invoked when performing particle-laden simulations is that of a monodisperse particle size distribution. In the present case, therefore, we target one largely unaddressed yet important aspect of particle-laden turbulence: characterizing the effects of polydispersity on wall-bounded turbulence modification. In this context, the present study aims at answering the following questions: Given a disperse (i.e. low-volume-fraction) mixture of particles with varying Stokes numbers, how can one characterize the turbulence modification observed? Are the effects additive, or does one particle size dominate the two-way interaction? Is there a single particle size that can represent the effects of the mixture? In answering these questions, we provide information which is essential for model and parameterization development for more realistic dispersed phase systems.

It is important to emphasize that by neglecting particle-particle interactions, the particles only interact indirectly through their modification to the carrier phase. Thus, the focus of this study is to determine the if mixtures of particles whose individual two-way coupling effects are understood can be represented by simply adding their effects — that is, can it be assumed that this indirect coupling between particles is small? While there are many physical systems which can be represented under this low volume concentration assumption, the simulations presented lend insight into the basic degree of coupling between distinct and separate scales of turbulent flow.

METHOD

For the class of flows of interest (e.g. large-scale geophysical flows), where particle/carrier phase density ratios are large and where volume fractions are small ($O(10^{-5})$ or less), the non-interacting point particle approximation is an appropriate model. We incorporate Lagrangian particles into direct numerical simulations of turbulent planar Couette flow, where two-way momentum coupling is enforced between the two phases.

Thus, an incompressible flow solver (Richter & Sullivan, 2013) is used to solve the (Eulerian) fluid and (Lagrangian) dispersed phase mass and momentum conservation equations:

$$\frac{\partial u_j}{\partial x_j} = 0, \tag{1}$$

$$\frac{\partial u_i}{\partial t} + u_j \frac{\partial u_i}{\partial x_j} = -\frac{1}{\rho_f}\frac{\partial p}{\partial x_i} + \nu_f \frac{\partial u_i}{\partial x_j^2} + \frac{1}{\rho_f} F_i. \tag{2}$$

$$\frac{dx_i}{dt} = v_i \tag{3}$$

$$\frac{dv_i}{dt} = \frac{f_i}{m_p} = \frac{g^*}{\tau_p}\left(u_{f,i} - v_i\right). \tag{4}$$

These equations govern the following dependent variables: u_i is the carrier phase (i.e. air) velocity, x_i is the particle location, v_i is the particle velocity, and p is the carrier phase pressure, solved via a Poisson equation to guarantee a divergence-free velocity field at each time step. ρ_f refers to the carrier phase density; ν_f is the carrier phase kinematic viscosity; $u_{f,i}$ is the carrier phase velocity interpolated using sixth-order Lagrange polynomials to the particle location; and τ_p is the particle acceleration timescale for Stokes flow around a cylinder: $\tau_p = \left(\rho_p/\rho_f\right) d_p^2/18\nu_f$, where ρ_p is the particle density and d_p is the particle diameter. m_p is the individual particle mass, and g^* is a Reynolds number correction to the Stokes drag on a sphere: $g^* = \left(1 + 0.15 Re_p^{0.687}\right)$, where $Re_p = |u_{f,i} - v_i| d_p/\nu_f$ is the particle Reynolds number (Clift *et al.*, 1978).

Two-way coupling is modeled via the F_i term in equation 2, which is computed by projecting the negative of the individual particle force f_i onto the surrounding computational nodes for every individual particle (Boivin *et al.*, 1998). By incorporating only a drag force on each particle (equation 4), it is assumed that the systems which these simulations represent have values of ρ_p/ρ_f which are large (Maxey & Riley, 1983). Similarly, since the volume fractions of the physical systems of interest are small (the simulations have volume fractions $\phi_V = O(10^{-4})$ or less), particle-particle collisions are neglected. Finally, gravity is also neglected to ensure the simplest possible interaction between the dispersed phase and surrounding turbulence.

The numerical solver is pseudospectral in the periodic streamwise (x) and spanwise (y) directions, and uses second-order finite differencing for spatial discretization in the wall-normal z direction. A low-storage, third-order Runge-Kutta scheme is used to integrate the equations in time (Spalart *et al.*, 1991). Additional details regarding the two-way coupled model and/or the numerical method can be found in Richter & Sullivan (2013).

The flow which is simulated is turbulent Planar Couette flow, which develops between two infinite, parallel planes moving in equal and opposite directions with a velocity of difference of U_0, separated by a distance H. The bulk Reynolds number of all simulations presented are $Re_b = U_0 H/\nu_f = 8000$ ($Re_\tau \approx 120$). Planar Couette flow is chosen instead of the more common channel flow because of two convenient properties: (1) the flow exhibits a constant total flux across the domain, making the modifications to Reynolds stresses unambiguous when comparing varying particle characteristics and (2) in addition to typical wall-bounded turbulent structures (hairpins, quasi-streamwise vortices, high/low speed streaks, etc.), Couette flow exhibits large streamwise structures characterized by an additional time and length scale with which the particles can interact (Tsukahara *et al.*, 2006; Pirozzoli *et al.*, 2014), thus providing a richer set of flow processes than can be found in channel flow. This latter feature is important in the context of polydisperse systems since particles will therefore preferentially concentrate on distinct spatial and temporal time scales depending on their inertia.

NUMERICAL EXPERIMENTS

We initially focus on three distinct particle sizes, with Stokes numbers (St_K based on the Stokes acceleration timescale and the centerline Kolmogorov timescale: $St_K = \tau_p/\tau_{K,centerline}$) of O(1), O(10), and O(100). In the simulations the Kolmogorov timescale varies roughly by a factor

of 5 between the centerline and the wall; we choose the centerline value because this is more easily obtained and reported in experimental investigations, but the general behavior from each of the three classes remains similar regardless of definition.

We choose these specific Stokes numbers particularly because the monodisperse behavior of each has been investigated in detail in past numerical studies (Richter & Sullivan, 2013, 2014; Richter, 2015), and each responds in a distinct way to the timescales available in the flow. In general, the $St_K = O(1)$ particles are most susceptible to preferential concentration at the scale of the near-wall streaks, and by themselves show the highest degree of carrier phase Reynolds stress attenuation. The $St_K = O(10)$ particles show a high degree of preferential concentration on the scales associated with the large-scale Couette structures, which yields an enhancement of streamwise velocity fluctuations but a reduction in Reynolds stress. The $St_K = O(100)$ particles remain homogeneously distributed throughout the domain and show similar changes in magnitude to the carrier phase Reynolds stresses as for $St_K = 10$.

In first set of simulations, binary mixtures are prescribed where the total constant dispersed phase mass fraction $\phi_m = 0.25$ is split into specific proportions. Due to limited space, only results from 50/50 mixtures, where 50% of the total particle mass comes from one particle type and the other 50% comes from a second, will be shown, but additional simulations have been done for 90/10 and 75/25 mixtures as well. 50/50 blends of each of the 3 combinations of $St_K = O(1)$, $St_K = O(10)$, and $St_K = O(100)$ are performed. Key simulations parameters are provided in table 1. In all simulations and for all Stokes numbers, the particle diameter is maintained constant at $d_p/H = 0.001$; the Stokes number is varied by modifying ρ_p.

Table 1. Simulation parameters for binary mixtures

Case	$St_{K,1}$	$St_{K,2}$	$N_{p,1}$	$N_{p,2}$	$\phi_{m,1}/\phi_{m,2}$
1	-	-	0	0	-
2	1	10	2.1e6	2.1e5	50/50
3	10	100	2.1e5	2.1e4	50/50
4	1	100	2.1e6	2.1e4	50/50

Finally, a continuous polydisperse simulation has also been performed, where particle Stokes numbers are chosen from a power law distribution of St_K ranging between $St_K = 1$ and $St_K = 100$. This is done by maintaining a constant particle diameter and choosing ρ_p to specify each Stokes number, and adding particles until the desired total mass fraction is attained.

RESULTS

To provide a qualitative illustration of the behavior of the simulated binary mixtures, as well as demonstrate the preferential concentration tendencies of the three magnitudes of St_K, figure 1 shows the instantaneous locations of each type of particle in the 50/50 mixtures of $St_K = O(1)$ and $O(10)$ particles (figure 1(a)) and $St_K = O(10)$ and $O(100)$ particles (figure 1(b)) at a horizontal plane located at $z/H = 0.1$. The descriptions above are seen clearly: $St_K = O(1)$ particles collect in small-scale, low-speed streaks, $St_K = O(10)$ particles collect in the larger-scale Couette upwelling regions, and $St_K = O(100)$ particles show no preferential concentration.

For the current discussion, the quantity of interest is the wall-normal momentum flux across the Couette cell. As mentioned above, a convenient feature of planar Couette flow is that momentum fluxes are uniform with height in this arrangement, and in the presence of a two-way coupled dispersed phase this constant total vertical momentum flux τ_{total} can be partitioned into three components:

$$\tau_{total} = \rho_f \left\langle u'w' \right\rangle - \rho_f \nu_f \frac{\partial \left\langle U \right\rangle}{\partial z} - \int_0^z \left\langle F_x(z^*) \right\rangle dz^*, \quad (5)$$

where the first term on the right hand side is the turbulent Reynolds stress, the second term is the viscous stress, and the third term is the particle stress. A momentum balance on the dispersed phase shows that the particle stress, which physically represents horizontal momentum of the particles being carried upwards by simultaneous vertical particle velocities, can be written in terms of the concentration-weighted dispersed phase Reynolds stress:

$$-\int_0^z \left\langle F_x(z^*) \right\rangle dz^* = \left\langle c \right\rangle \left\langle u'_p w'_p \right\rangle_c, \quad (6)$$

where u'_p and w'_p are fluctuating particle velocities, c is the dispersed phase mass concentration, and the brackets with subscript "c" refer to a mass-weighted average only over the particle phase.

Figure 2(a) shows the vertical profiles of the stress components, each normalized with $\rho_f U_0^2$ for several of the binary mixtures. The black curves show the momentum fluxes for an unladen case for comparison. As expected, the particle stress for the unladen case is zero, and the turbulent Reynolds stress represents nearly all of the total stress near the channel center.

For sake of brevity, figure 2 shows only the cases with the 50/50 blends of particles. Figure 2(a) shows that for each of these three cases, the turbulent Reynolds stress decreases to a similar degree, which is nearly offset by a rise in the particle stress. The two cases which include $St_K = O(1)$ particles (red and blue) have nearly identical particle stresses, while the case which contains $St_K = O(10)$ and $St_K = O(100)$ particles shows a small but systematic difference both in the Reynolds stress and particle stress profiles.

This tradeoff between the turbulent flux of momentum and the particle stress has been studied extensively for monodisperse systems (Richter & Sullivan, 2013, 2014; Richter, 2015), and at this low Reynolds number results from momentum exchange between the particles and near-wall motions. Turbulent ejection events carrying low-momentum fluid are instead weakened by the acceleration and vertical "launching" of inertial particles (thus reducing the Reynolds stress through sharp reductions in w'), and the vertical movement of these horizontally-moving particles represents the vertical momentum transport that would have been performed by the Reynolds stress in unladen conditions.

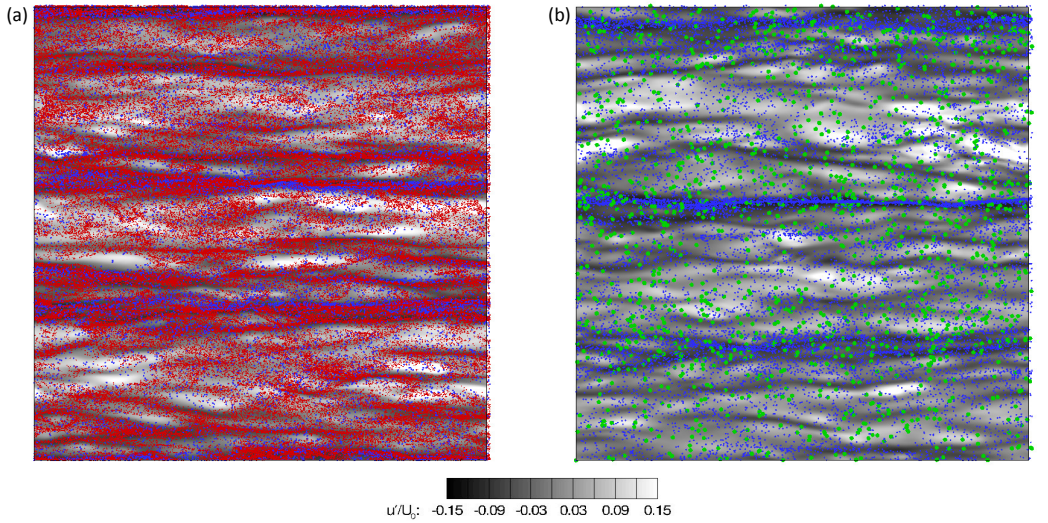

Figure 1. Instantaneous horizontal slices of nondimensional streamwise velocity fluctuation u'/U_0 (black and white contours; see legend) at $z/H = 0.1$. (a) 50/50 mixture of (red) $St_K = O(1)$ and (blue) $St_K = O(10)$ particles; (b) 50/50 mixture of (blue) $St_K = O(10)$ and (green) $St_K = O(100)$ particles. Particle sizes are not to scale but are weighted to emphasize differences in particle mass.

As mentioned above, the effectiveness of the particles to reduce the Reynolds-stress-causing motions is maximized for $St_K = O(1)$ due to the inability of more inertial particles to collect in regions where they can most efficiently damp near-wall ejection motions (Richter & Sullivan, 2014). Thus the interactions expected in the present simulations are only due to one particle type modifying the flow in a way which modifies the second type's ability to modify these motions (as opposed to particle collisions modifying the regions of preferential accumulation).

With this in mind, figures 2(b–d) show the total particle stress for each of the cases (solid line), broken down into individual stresses resulting from each particle type contained in the mixture (dashed and dotted lines). As expected from previous monodisperse simulations, the $St_K = O(1)$ particles carry nearly twice as much stress as either $St_K = O(10)$ or $St_K = O(100)$ particles when combined in the mixture (figures 2(b) 2(c)). The mixture of $St_K = O(10)$ and $St_K = O(100)$ particles shows that each carries roughly the same amount of momentum, which again is expected from monodisperse simulations.

More interestingly, it is found that the momentum carried by the dispersed phase is nearly additive for these mixtures, indicating that the changes to turbulence due to one sized particle does not change the ability of the other particle to interact and modify turbulence at the same time. To show this, monodisperse simulations were performed where the total mass loading was half of the total in the current cases. Then, figures 2(b–d) demonstrate with the dash-dotted line that the sum of these independent, monodisperse particle stress profiles leads to a total stress which is nearly identical to the total stress computed in the mixture cases. This is generally true at all heights across the channel, and the only minor deviations (which represent the presence of one particle type modifying the two-way coupling of the other) occur near the peak of the particle stress around $z/H \approx 0.1$.

In some sense, this is not surprising since the particles do not directly interact with each other and since the particles respond to flow timescales differing by an order of magnitude, yet it has favorable modeling implications since their reductions to the carrier phase Reynolds stress are linear and additive. This then begs the question: for a continuous distribution of particle mass (as opposed to binary mixtures), does this linearity still hold, and is there an effective monodisperse particle mass which can represent the entire system?

A final simulation is performed where the particle mass, specified by the particle density where all particles have equal radii, is distributed according to a power law distribution at the same total dispersed has mass loading as in the previous cases. The Stokes numbers of the particles are thus also distributed according to a power law distribution, chosen to vary between a minimum of $St_K \approx 1$ to $St_K \approx 100$, as seen in figure 3(a). By enforcing a power law distribution of the particle mass, each particle mass bin contributes equally to the overall total mass (as a percentage).

Figure 3(b) then shows that the resulting particle stress is similar in magnitude to the binary $St_K = O(10)$ and $O(100)$ mixture. This can be explained by examining figures 2(b–d), where it it is noticed that the $St_K = O(10)$ and $St_K = O(100)$ particles, while possessing very different clustering properties, exhibit overall particle stresses quite similar to one another. More importantly, these similar particle stresses are distinct from and much less than those resulting from $St_K = O(1)$ particles, which dominate whichever binary mixture they find themselves a part of.

Thus, it appears that, at least for the range of $1 < St_K < 100$ tested presently, particles with Stokes numbers of 10 and larger have saturated in their ability to carry momentum across the domain (primarily due to their increasing inability to preferentially concentrate), and thus the contribution from any particles above $St_K \approx 10$ is more or less similar (see figure 2(d) in particular). Hence, the polydisperse blend, which has nearly 90% of its total mass resulting from particles with $St_K > 10$, appears very similar to the $St_K = O(10)/O(100)$ binary mixture, indicating that there are two general "classes" or particles in this wall-bounded

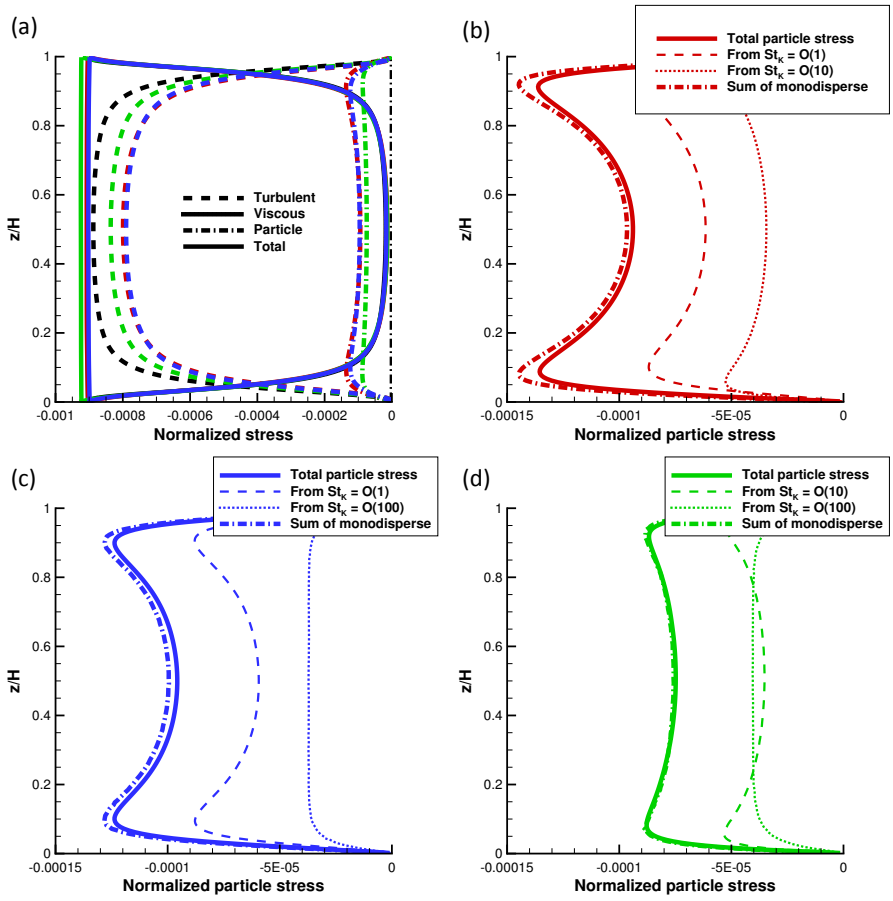

Figure 2. Stress plots for 50/50 blend simulations: black: unladen; red: $St_K = O(1)$ and $St_K = O(10)$; blue: $St_K = O(1)$ and $St_K = O(100)$; green: $St_K = O(10)$ and $St_K = O(100)$. (a): All stress profiles (turbulent, viscous, particle-induced, and total components) responsible for carrying momentum across the domain. With varying binary mixtures of particles, the carrier phase Reynolds stress decreases, which is offset by a rise in the particle stress. Mixtures involving $St_K = O(1)$ particles exhibit the largest effect. (b-d): The total particle stress and the individual contribution from each particle size. The total particle stress is compared to the linear sum of the total particle stress from two monodisperse simulations with the same number of each size particle.

flow: those which have timescales of similar order to the motions responsible for turbulent Reynolds stresses (e.g., $St_K = O(1)$ here), and those which are larger. The first class exhibits the bulk of the total available particle stress, while the second contributes more or less similar results for a very wide range of particle mass.

Finally, revisiting the previous question regarding an effective particle diameter, the right hand side of equation 6 can be used to relate the particle stress of the polydisperse system to the particle stress if each particle had some equal mass $m_{p,eff}$:

$$m_{p,eff} = \frac{\langle c \rangle \langle u'_p w'_p \rangle_c}{\langle n \rangle \langle u'_p w'_p \rangle_n}, \tag{7}$$

where n is the number concentration and the subscript $\langle \cdot \rangle_n$ refers to the arithmetic mean throughout elements of the dispersed phase. As computed in equation 7, $m_{p,eff}$ is a function of z. When computing this quantity for the polydisperse simulation, it is found that its value varies very little with height, and that its vertically averaged value corresponds to a particle with Stokes number of $St_{K,eff} = 19$. This value of $St_K = 19$ is remarkably close to the Stokes number of a particle merely corresponding to the mean of the power law distribution: $\langle St_K \rangle = 21$, thus again suggesting the linearity of the particle stresses in the simulated system.

CONCLUSIONS

It is important to emphasize the underlying assumption of low volume concentration used throughout this study, since in the limit of dense suspensions particle-particle collisions will clearly lead to nonlinearities and couplings between the stresses carried by each particle size. The present results therefore pertain only to physical systems where particle stresses are non-negligible (i.e., moderate mass loading), while volume concentrations remain low — for example dust or droplet suspensions in air.

The current study shows that in these flows, the individual stress carried by each class size of particle contributes independently to the overall particle stress, which has quite favorable consequences in terms of modeling the full polydisperse system. Since the particles do not interact,

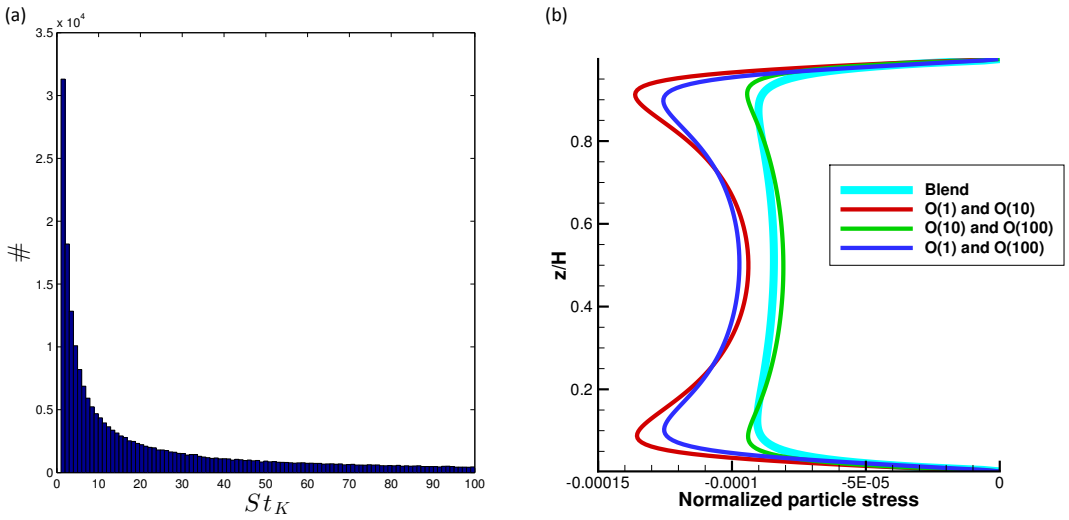

Figure 3. (a) Histogram of the particle Stokes numbers throughout the continuous polydisperse simulation, ranging from $St_{K,min} \approx 1$ to $St_{K,max} \approx 100$. All particles sum to a total mass loading of $\phi_m = 0.25$. (b) Particle stress profiles for the binary mixtures, as well as the polydispersed blend (cyan).

this implies that each class' effect on the turbulence does not greatly impede the ability of other sizes to interact with the flow, and this is particularly true when considering particles with timescales near that of the Reynolds-stress-containing motions versus those that are larger. The appealing linearity of the particle stresses therefore indicates that modeling through an effective particle mass may be feasible for systems adhering to the aforementioned assumptions.

REFERENCES

Andreas, Edgar L. 2011 Fallacies of the enthalpy transfer coefficient over the ocean in high winds. *Journal of the Atmospheric Sciences* **68**, 1435–1445.

Balachandar, S. & Eaton, John K. 2010 Turbulent dispersed multiphase flow. *Annual Review of Fluid Mechanics* **42**, 111–133.

Bao, J.-W., Fairall, Christopher W., Michelson, S. A. & Bianco, L. 2011 Parameterizations of sea-spray impact on the airsea momentum and heat fluxes. *Monthly Weather Review* **139**, 3781–3797.

Bennett, Sean J., Atkinson, Joseph F., Hou, Yinting & Fay, Michael J. 2013 Turbulence modulation by suspended sediment in a zero mean-shear geophysical flow. In *Coherent Flow Structures at Earth's Surface* (ed. Jeremy G. Venditti, James L. Best, Michael Church & Richard J. Hardy), chap. 20, pp. 309–321. John Wiley and Sons.

Boivin, Marc, Simonin, Olivier & Squires, Kyle D. 1998 Direct numerical simulation of turbulence modulation by particles in isotropic turbulence. *Journal of Fluid Mechanics* **375**, 235–263.

Clift, Roland, Grace, John R. & Weber, Martin E. 1978 *Bubbles, Drops, and Particles*. Academic Press.

Ferrante, Antonino & Elghobashi, Said 2003 On the physical mechanisms of two-way coupling in particle-laden isotropic turbulence. *Physics of Fluids* **15** (2), 315–329.

Gore, R. A. & Crowe, Clayton T. 1989 Effect of particle size on modulating turbulent intensity. *International Journal of Multiphase Flow* **15** (2), 279–285.

Kulick, Jonathan D., Fessler, John R. & Eaton, John K. 1994 Particle response and turbulence modification in fully developed channel flow. *Journal of Fluid Mechanics* **277**, 109–134.

Maxey, Martin R. & Riley, James J. 1983 Equation of motion for a small rigid sphere in nonuniform flow. *Physics of Fluids* **26** (4), 883–889.

Pirozzoli, Sergio, Bernardini, Matteo & Orlandi, Paolo 2014 Turbulence statistics in Couette flow at high Reynolds number. *Journal of Fluid Mechanics* **758**, 327–343.

Richter, David H. 2015 Turbulence modification by inertial particles and its influence on the spectral energy budget. *Physics of Fluids* p. Under Review.

Richter, David H. & Sullivan, Peter P. 2013 Momentum transfer in a turbulent, particle-laden Couette flow. *Physics of Fluids* **25**, 053304.

Richter, David H. & Sullivan, Peter P. 2014 Modification of near-wall coherent structures by inertial particles. *Physics of Fluids* **26**, 103304.

Spalart, Philippe R., Moser, Robert D. & Rogers, Michael M. 1991 Spectral methods for the Navier-Stokes equations with one infinite and two periodic directions. *Journal of Computational Physics* **96**, 297–324.

Tanaka, Tomohiko & Eaton, John K. 2008 Classification of turbulence modification by dispersed spheres using a novel dimensionless number. *Physical Review Letters* **101**, 114502.

Tsukahara, Takahiro, Kawamura, Hiroshi & Shingai, Kenji 2006 DNS of turbulent Couette flow with emphasis on the large-scale structure in the core region. *Journal of Turbulence* **7** (19), 1–16.